PLOS | ONE

RESEARCH ARTICLE

Two Half-Sandwiched Ruthenium (II) Compounds Containing 5-Fluorouracil Derivatives: Synthesis and Study of DNA Intercalation

Zhao-Jun Li[1], Yong Hou[2], Da-An Qin[3], Zhi-Min Jin[4]*, Mao-Lin Hu[3]*

1 Institute of Agricultural Resources and Regional Planning, Chinese Academy of Agricultural Sciences, Key Laboratory of Plant Nutrition and Fertilizer, Ministry of Agriculture, Beijing, China, **2** Institute of Biotechnology and Nucleic Technology, Sichuan Academy of Agricultural Sciences, Chengdu, China, **3** College of Chemistry and Materials Engineering, Wenzhou University, Wenzhou, China, **4** College of Pharmaceutical Sciences, Zhejiang University of Technology, Hangzhou, China

* zimichem@sina.com (ZMJ); maolin@wzu.edu.cn (MLH)

Citation: Li Z-J, Hou Y, Qin D-A, Jin Z-M, Hu M-L (2015) Two Half-Sandwiched Ruthenium (II) Compounds Containing 5-Fluorouracil Derivatives: Synthesis and Study of DNA Intercalation. PLoS ONE 10(3): e0120211. doi:10.1371/journal.pone.0120211

Academic Editor: Heidar-Ali Tajmir-Riahi, University of Quebect at Trois-Rivieres, CANADA

Received: November 4, 2014

Accepted: January 20, 2015

Published: March 19, 2015

Data Availability Statement: All relevant data are within the paper and its Supporting Information files.

Funding: This work was jointly supported by the Natural Science Foundation of Institute of Agricultural Resources and Regional Planning, Chinese Academy of Agricultural Sciences (Project No. 2014-3; website: http://www.iarrp.cn) and the special projects foundation of Beijing Municipal Science & Technology Commission (Z141105000614012). This research was also supported by the Natural Science Foundation of China (Nos. 21071111 and 21371137); website: http://www.nsfc.gov.cn (Nos. 21071111 and 21371137). The funders had no role in study design,

Abstract

Two novel coordination compounds of half-sandwiched ruthenium(II) containing 2-(5-fluorouracil)-yl-N-(pyridyl)-acetamide were synthesized, and their intercalation binding modes with calf thymus DNA were revealed by hyperchromism of ultraviolet-visible spectroscopy; the binding constants were determined according to a *Langmuir* adsorption equation that was deduced on the base of careful cyclic voltammetry measurements. The two compounds exhibited DNA intercalation binding activities with the binding constants of 1.13×10^{6} M^{-1} and 5.35×10^{5} M^{-1}, respectively.

Introduction

Cisplatin shows a strong ability of binding to and causing crosslinking of DNA in *vivo*, which ultimately triggers cell apoptosis, and is used successfully to treat some special types of cancers. The discovery of cisplatin has aroused great effort toward the design of metal-based anticancer drugs [1]. Particular interest is attracted toward ruthenium element, a member of platinum-group, due to its low toxity and its ability to mimic iron in binding with proteins in the plasma [2]. In the recent decades, as a potential anticancer medicine, organometallic ruthenium compounds of the type [Ru(η^6-arene)] are under intensive investigation, owing to their promising activity in *vitro* and in *vivo* toward cancer cell, including cisplatin-resistant cells [3].

Combining two or more multifunctionalities into one is a popular strategy in design new therapeutic agents. 5-Fluorouracil (5-FU) has been used extensively in the treatment of solid tumors for years, and in the late, its strong toxicities to the gastric system, intestinal mucosa and bone marrow is evidenced eventually. Therefore, attempts are made to improve its anticancer activity and to minimize its side effects by exploiting several prodrug, such as amines, alcohols, and peptides [4]. In the literature, covalent compound containing platinum(II) and 5-FU

data collection and analysis, decision to publish, or preparation of the manuscript.

Competing Interests: The authors have declared that no competing interests exist.

fragment has been reported [5], but covalent compound containing ruthenium and 5-FU fragment is not available.

The interaction of DNA with small molecule had been a hot subject of research [6–11] for long time, due to the interaction modes and kinetic mechanism reflected various senses for developing molecular drugs and probers to monitor DNA structure [12–15]. In this respect, we synthesized two novel half-sandwiched ruthenium(II) compounds from dichloro(p-cymene) ruthenium(II) dimer and 2-[(5-fluorouracil)-yl]-N-pyridyl-acetamide for the first time, and studied the interaction of calf thymus DNA (CT-DNA) with them by cyclic voltammetry and UV-vis spectrometry.

Experimental

1. Apparatus and reagents

CT-DNA with high molecular weight was extracted and purified by a method described elsewhere [16]. All other chemicals, including dichloro(p-cymene)ruthenium(II) dimer {$[(\eta^6$-*p*-cymene)$RuCl_2]_2$} and 5-FU, were of analytical reagent grade, and were purchased from sigma-aldrich Co. (USA).

The CT-DNA solution was prepared with 0.1 M KCl / 0.05 M Tris—HCl (pH 7.16) and stored at 4°C. The concentration of DNA was determined by UV absorbance at 260 nm, with the extinction coefficient (ε_{260}) taken as 6600 $M^{-}1\ cm^{-1}$.

The electrochemical measurements were performed on a CHI1030b electrochemical workstation (CH Instrumental, Chenhua Corp., Shanghai, China). Supporting electrolyte for all experiments was a 0.1 M KCl / 0.05 M Tris—HCl buffer solution, which was adjusted to pH 7.16 by HCl.

IR spectra were recorded on an EQUINOX-55 instrument (Bruker Optics, Germany). Elemental analysis was performed on a Perkin-Elmer 2400 CHNS/O elemental analyzer (USA). The UV-vis spectra were recorded at room temperature on a U-3010 spectrophotometer (Hitachi, Japan) equipped with 1.0 cm quartz cells. ^{1}HNMR and ^{13}CNMR spectra were recorded on a AVANCE-500 instrument using tetramethylsilane (TMS) as an internal standard at room temperature, and the chemical shifts were given in relative to TMS.

2. Synthesis of Ruthenium compounds I and II

Two isomeric 5-FU derivatives, 2-[5-fluoro-2,4-dioxo-3,4-dihydropyrimidin-1(2H)-yl]-N- (pyridin-2-yl)-acetamide (L1) and 2-[5-fluoro-2,4-dioxo-3,4-dihydropyrimidin-1(2H)-yl]-N-(pyridin- 3-yl)-acetamide (L2), were synthesized (Fig. 1) in accordance with a procedure described previously [17]. The two titled compounds were synthesized from the 5-FU derivative and dichloro(p-cymene)ruthenium(II) dimer. Typically, 2-[(5-fluorouracil)-yl]-N-pyridyl-acetamide (66 mg, 0.25 mmol) was added dropwise to a suspension of $[(\eta^6$-cymene)$RuCl_2]_2$ (76.5 mg, 0.125 mmol) in freshly distilled anhydrous methanol (25 mL). The color of the resulting mixture changed immediately with stirring at 25°C under argon, and precipitate was formed after storage in a freezer at -18°C for 24 h. The fine yellow solid was collected by filtration, recrystallized from methanol/ether, washed with methanol followed by ether, and dried overnight in vacuo.

$$[(\eta^6 - p - \text{cymene})\text{Ru(L1)Cl}_2] \quad \text{(I)}$$

Yield based on $[(\eta^6$-cymene)$RuCl_2]_2$: 54.4%. IR: 3390 (υ N-H), 3291, 3044 (υ C-H), 2843 (υ-CH_2-), 1705 (υ C = O), 1479 (υ C-N), 1430, 1375, 1234 (υ C-F), 879, 763, 686 cm^{-1} (S1 Fig.). Anal. calc. for $C_{20}H_{23}Cl_2FN_4O_3Ru$ (558.37), C 43.02% N 10.03% H 4.15%; found: C42.98%

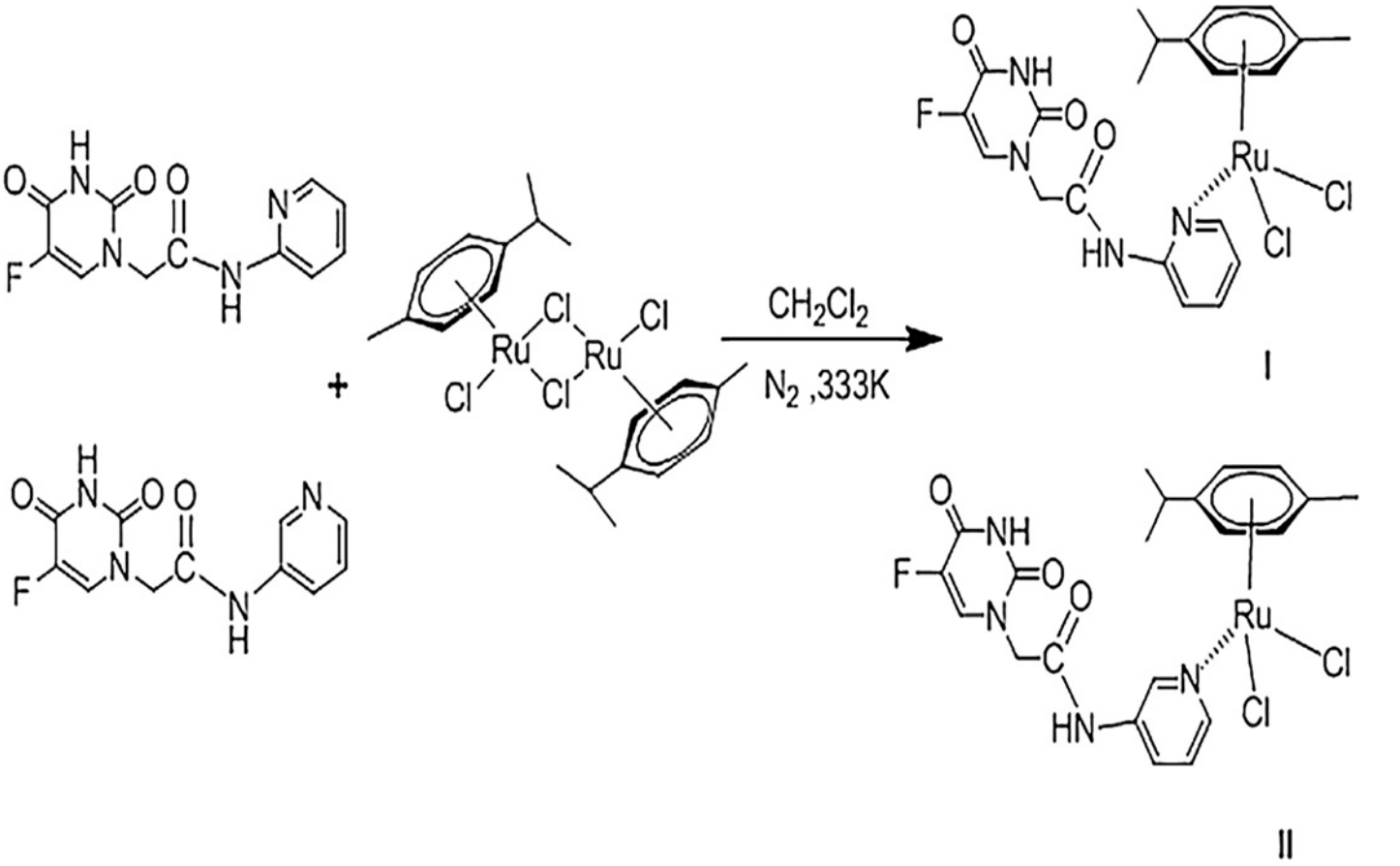

Fig 1. Synthetic routes of compound I and II.

doi:10.1371/journal.pone.0120211.g001

N 10.11% H 4.10%. ^{1}HNMR (500 MHz, DMSO-d_6) δ: 11.96 (1H, s), 8.11 (1H, d, J = 6.8 Hz), 7.90 (1H, dd, J = 5.1, 1.0 Hz), 7.43 (1H, ddd, J = 8.8, 7.2, 1.9 Hz), 6.51 (1H, d, J = 3.5 Hz), 6.49 (1H, d, J = 3.5 Hz), 5.84 (2H, d, J = 6.3 Hz), 5.80 (2H, d, J = 6.3 Hz), 4.36 (2H, s), 2.84 (1H, dt, J = 13.8, 6.9 Hz), 2.10 (3H, s), 1.20 (6H, d, J = 6.9 Hz) ppm (S2 Fig.). 13C NMR (126 MHz, DMSO-d_6) δ: 169.49 (s), 159.10 (s), 157.47 (d, J = 25.8 Hz), 149.67 (s), 146.23 (s), 139.28 (d, J = 228.6 Hz), 137.78 (s), 111.77 (s), 108.62 (s), 106.37 (s), 100.09 (s), 85.95 (d, J = 107.1 Hz), 48.78 (s), 29.98 (s), 21.51 (s), 17.88 (s) ppm (S3 Fig.).

$$[(\eta^6 - p - \text{cymene})\text{Ru(L2)Cl}_2] \quad \text{(II)}$$

Yield based on $[(\eta^6\text{-cymene})\text{RuCl}_2]_2$: 61.3%. IR: 3520 (υ N-H), 3256, 3050 (υ C-H), 2926 (υ-CH_2-), 1704 (υ C = O), 1485 (υ C-N), 1430, 1381, 1220 (υ C-F), 809, 694 cm^{-1} (S4 Fig.). Anal. calc. for $C_{20}H_{23}Cl_2FN_4O_3Ru$ (558.37), C 43.04% N 10.04% H 4.18%; found: C 43.02% N 10.03% H 4.15%. ^{1}HNMR (500 MHz, DMSO-d_6) δ: 11.95 (1H, d, J = 5.0 Hz), 10.54 (1H, s), 8.72 (1H, d, J = 2.2 Hz), 8.29 (1H, d, J = 3.6 Hz), 8.11 (1H, d, J = 6.7 Hz), 8.06–7.97 (1H, m), 7.37 (1H, dd, J = 8.3, 4.7 Hz), 5.82 (2H, d, J = 6.3 Hz), 5,78 (2H, d, J = 6.3 Hz), 4.53 (2H, s), 2.83 (1H, dt, J = 13.7, 6.9 Hz), 2.08 (3H, s), 1.19 (6H, d, J = 6.9 Hz) ppm (S5 Fig.). 13C NMR (126 MHz, DMSO-d_6) δ:165.98 (s), 157.50 (d, J = 25.6 Hz), 149.77 (s), 144.60 (s), 140.43 (d, J = 64.6

Hz), 138.36 (s), 135.16 (s), 131.01 (d, J = 34.0 Hz), 126.14 (s), 123.77 (s), 106.38 (s), 100.08 (s), 85.92 (d, J = 106.7 Hz), 50.14 (s), 29.95 (s), 21.48 (s), 17.84 (s) ppm (S6 Fig.).

3. Preparation of (CT-DNA)-modified electrode

The electrodes were modified with CT-DNA in a procedure reported previously [18, 19]. Gold disk electrodes were polished with a series of alumina powder (1.0, 0.5 and 0.05 μm), then was purified and placed in fresh piranha solution (30% H_2O_2 and 70% H_2SO_4) to remove adsorbed organic impurities and sonicated in highly purified water for 5 min. Prior to the modification, the electrode surface was electrochemically activated by sweeping from -0.3 to +1.5 V in 0.1 M H_2SO_4 solution until a stable cyclic voltammogram characteristic of a clean gold electrode was obtained. After being washed with twice-distilled water, the freshly polished gold electrode was immediately modified by transferring a droplet of 10 μL of 1.0 μg μL^{-1} CT-DNA solution onto its surface, followed by air-drying overnight. The CT-DNA-modified electrode (CT-DNA/Au) was then soaked in sterile water for about 4 h and rinsed with water to remove unadsorbed CT-DNA.

4. Cyclic voltammetry

Voltammetric measurements were carried out in a conventional cell consisting of three-electrode, namely a bare gold (or CT-DNA/Au) as the working electrode, a saturated calomel electrode, and a platinum wire auxiliary electrode. A CT-DNA/Au electrode was soaked in buffer solution with different concentrations of the compound for voltammetric test designed to investigate the interaction of CT-DNA. Typical cyclic voltammetry experiment was carried out in a 5 mM solution of $K_3[Fe(CN)_6]$ / $K_4[Fe(CN)_6]$ (1:1) in the supporting electrolyte at room temperature (25°C). All solutions were deaerated with highly pure nitrogen, and the electrochemical experiments were performed at a scan rate of 0.1 Vs^{-1}.

5. UV-visible spectra

The UV-vis spectrum was performed in 0.1 M KCl / 0.05 M Tris—HCl buffer at pH 7.16 and a temperature of 25°C, in the wavelength range of 200–600 nm. The concentration of CT-DNA was kept constant and the concentrations of two compounds were ranged from 0.04 mM to 0.20 mM.

Results and Discussion

1. Electrochemical characterization of CT-DNA-modified electrode

Transition-metal compounds were often applied to probe both structural and functional aspects of DNA [20–21]. In this study, $Fe(CN)_6^{3-/4-}$ was used as an electrochemical probe molecule to characterize the interaction of DNA with the two titled compounds. As shown in Fig. 2, the cyclic voltammogram showed a couple of well-defined redox waves at bare gold with a peak-to-peak separation of 70 mV (curve a), and at CT-DNA/Au with such peak separation of 108 mV (curve b). Compared with curve *a*, the redox peak of curve *b* current decreased obviously. This indicated that CT-DNA had been assembled successfully on Au surface, and that CT-DNA acted as inert electron and mass transfer blocking layer and thus hindered the diffusion of ferricyanide towards the electrode surface. Further, the cyclic voltammogram of the same CT-DNA electrode remained stable after 20 scans in Tris-HCl buffer solution, suggesting high electrochemical stability of the DNA-coated film.

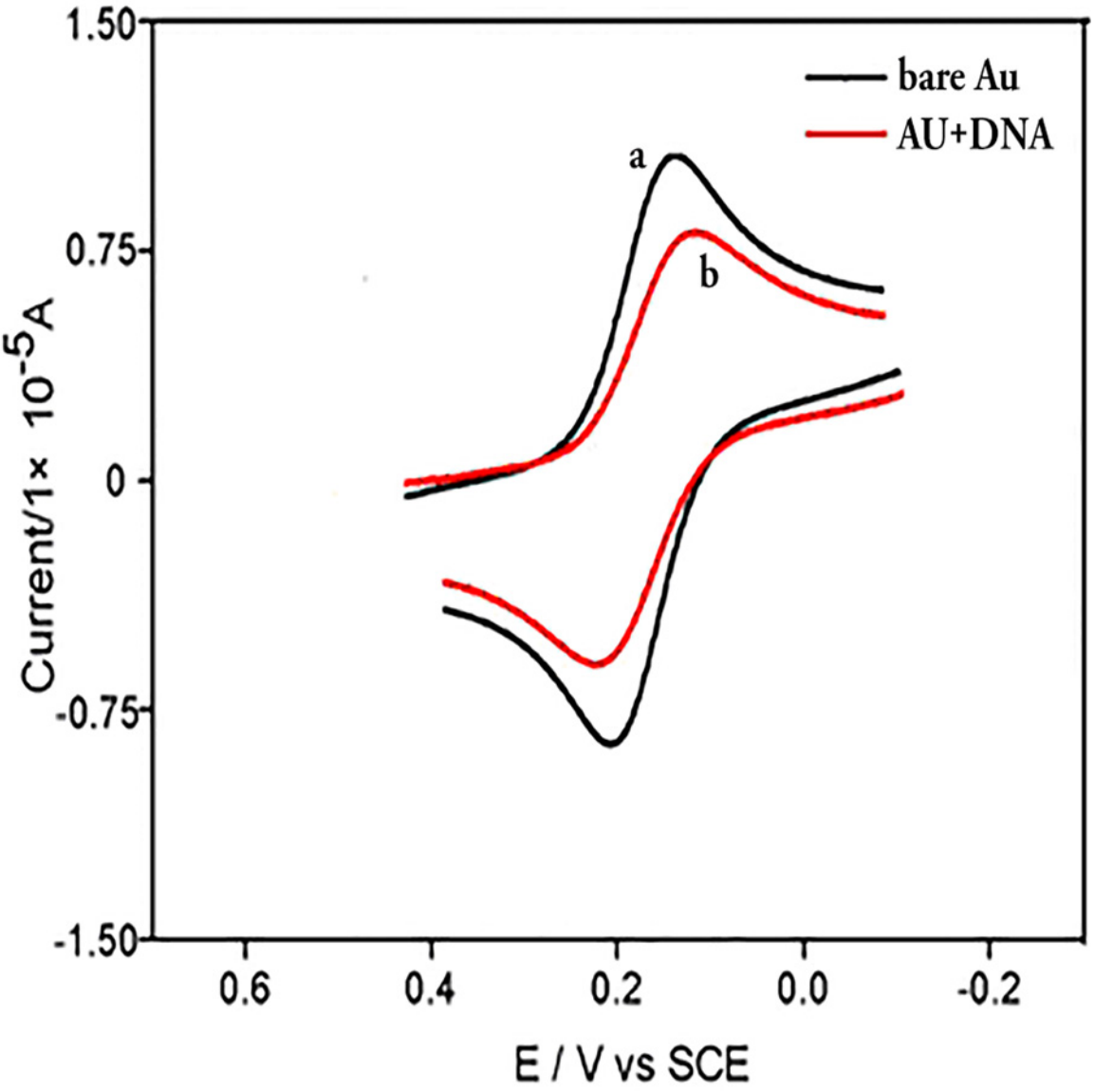

Fig 2. Cyclic voltammograms of $Fe(CN)6^{3-/4-}$ in pH 7.16 Tris—HCl buffer solution at a bare Au electrode (a) and CT-DNA/Au (b), respectively. The scan rate was 0.1 V s^{-1} and the concentrations of $Fe(CN)_6^{3-/4-}$ and KCl were 5 mM.

doi:10.1371/journal.pone.0120211.g002

2. Interaction of the compounds with CT-DNA-modified gold electrode

As was shown in Fig. 3, the peak current of $Fe(CN)_6^{3-/4-}$ decreased as compounds (I or II) were added into the test solution. The more compound was added, the more the peak current of probe molecule decreased. As shown in Fig. 4, both peak currents of the cyclic voltammograms decreased with the concentrations of compounds increasing and tended to achieve a saturation value, i.e. at about 0.60 mM, as expected according to *Langmuir* adsorption behaviour. The reason might be attributed to that CT-DNA films made the redox process of $Fe(CN)_6^{3-/4-}$ at the gold electrode more difficult due to the physical blockage as well as possible electrostatic

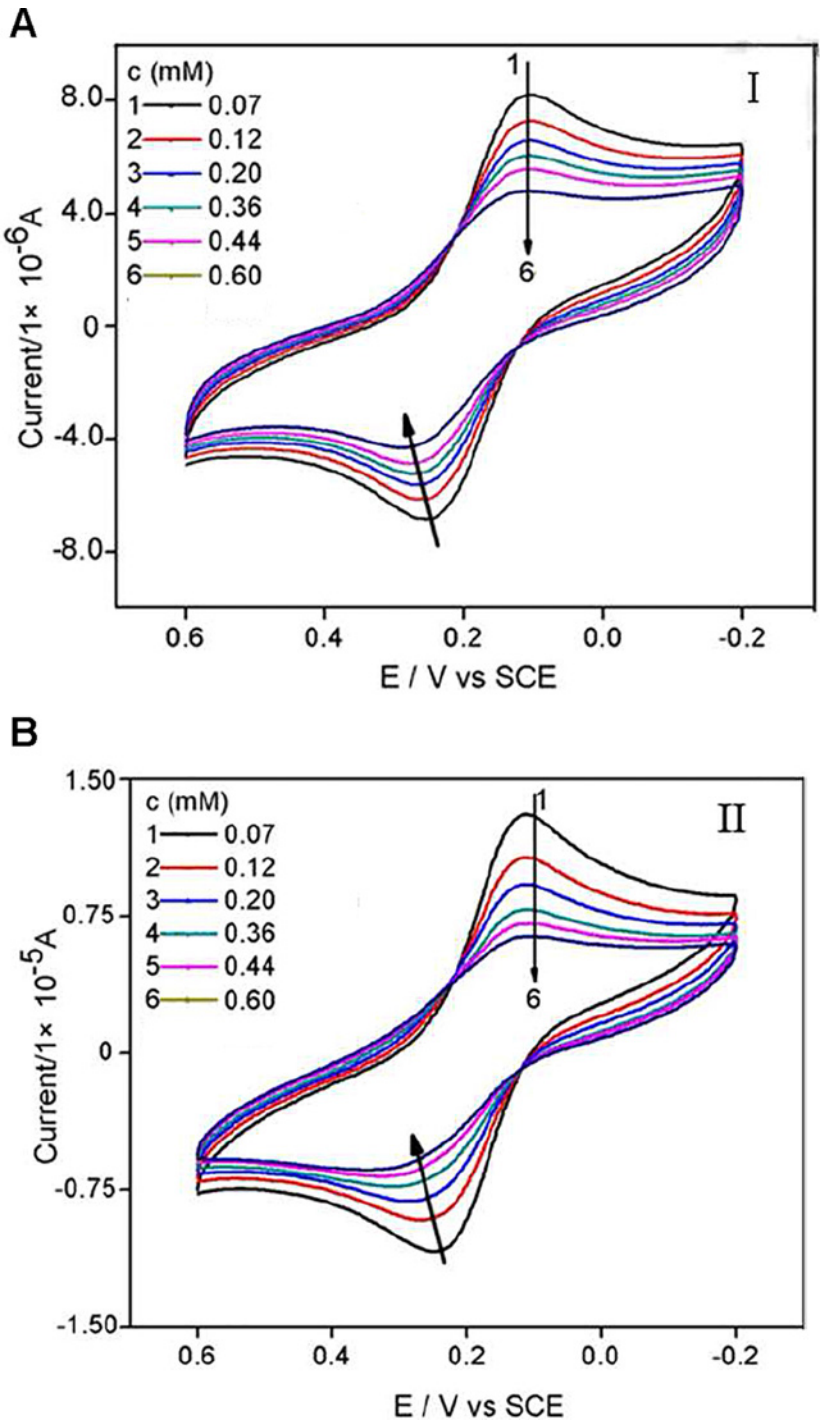

Fig 3. Cyclic voltammograms of $Fe(CN)6^{3-/4-}$ in Tris—HCl buffer solution (pH 7.16) containing different concentrations of compound I and II. The scan rate was 0.1 V s-1 and the concentrations of $Fe(CN)_6^{3-/4-}$ and KCl were 5 mM.

doi:10.1371/journal.pone.0120211.g003

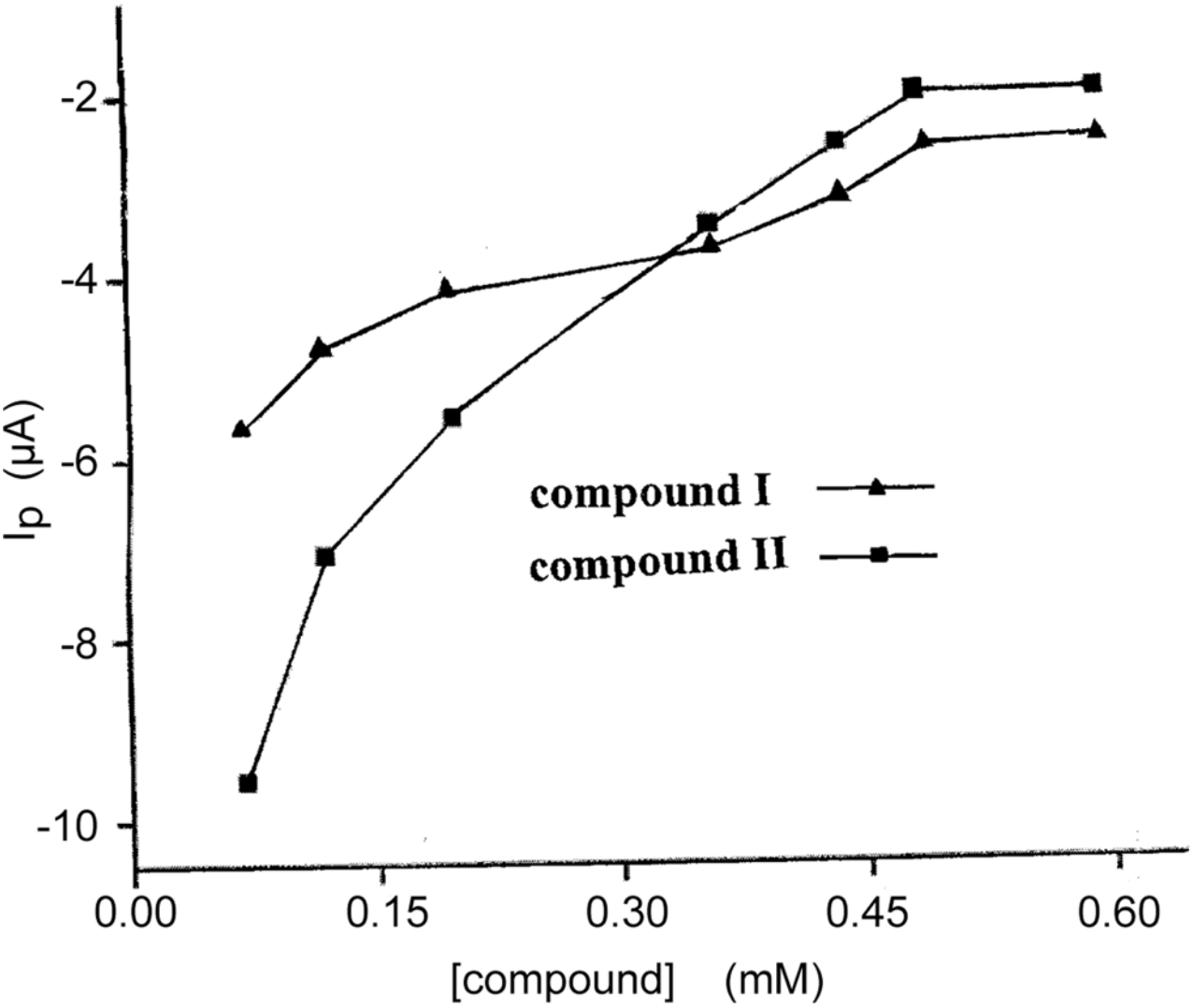

Fig 4. The dependence of decrease value of the peak current on the concentration of compound I and II.

doi:10.1371/journal.pone.0120211.g004

repulsion, and that the addition of the two compounds to the solution caused the CT-DNA film denser due to molecular interaction, therefore harder for $Fe(CN)_6^{3-/4-}$ ions to migrate through.

According to a previously reported method [22, 23], it was assumed that CT-DNA and DRUG produced a single complex of $DNA{\cdot}DRUG_m$ only.

$$DNA + m\ DRUG \leftrightarrow DNA \cdot DRUG_m \tag{1}$$

The constant (K) was descripted as follows:

$$K = \frac{[DNA \cdot DRUG_m]}{[DNA] \cdot [DRUG]^m} \tag{1.1}$$

And the following equations could be deduced, where I indicated cyclic voltammetry current.

$$\Delta I_{MAX} = k' \cdot C_{DNA} \tag{1.2}$$

$$\text{and } \Delta I = k' \cdot [DNA \cdot DRUG_m] \tag{1.3}$$

$$[DNA] + [DNA \cdot DRUG_m] = C_{DNA} \tag{1.4}$$

$$\Delta I_{max} - \Delta I = k'(C_{DNA} - [DNA \cdot DRUG_m]) \tag{1.5}$$

$$\Delta I_{max} - \Delta I = k' \cdot [DNA] \tag{1.6}$$

As equations (1.3) and (1.6) were put into (1.1), it yielded:

$$\log \frac{\Delta I}{\Delta I_{max} - \Delta I} = \log K + m \log[DRUG] \tag{1.7}$$

$$\frac{1}{\Delta I} = \frac{1}{\Delta I_{max}} + \frac{1}{\Delta I_{max} \cdot K} \cdot \frac{1}{[DRUG]^m} \tag{1.8}$$

As for Equation (1.8), we assumed $m = 1$, using ΔI_P to represent ΔI, and $\Delta I_{p,\,max}$ to represent ΔI_{max}. As shown in Fig. 5, 1/[DRUG] demonstrated a good linear relationship with $1/\Delta I_p$, indicating reasonable assumptive value of m for compounds I and II. Thus, the equation (1.9) was deduced [24], where $\Delta I_p = I_p\text{-}I_{po}$, I_p and I_{po} represent the oxidation peak current of $Fe(CN)_6^{3-/4-}$ in the presence and absence of the drugs, respectively; $\Delta I_{p,max}$ was the maximum difference of the oxidation peak current; and [DRUG] represented the concentration of the drug.

$$\frac{1}{\Delta I_p} = \frac{1}{\Delta I_{p,max}} + \frac{1}{\Delta I_{p,max} \cdot K} \cdot \frac{1}{[DRUG]} \tag{1.9}$$

The binding constant (K) between the compounds and CT-DNA, 1.13×10^6 M^{-1} and 5.35×10^5 M^{-1} for compound I and II respectively, was calculated according to the equation (1.9). These values were typical for metal compounds that bind to DNA via intercalation mode [25]. The binding constant of compound I was about 2.1 times larger than that of compound II, which indicated that the CT-DNA-binding strength of compound I was stronger than that of compound II. A stronger bonding indicated a more stable combination with CT-DNA and thus a better anticancer activity [26].

3. Ultraviolet-visible absorbance spectra

Generally, the DNA double-helix structural change, which is caused by its binding with other molecules, may be revealed in spectral features of hyperchromism (rise in absorption intensity) and hypochromism (fall in absorption intensity). The hyperchromism arises from disassembling of DNA double strand [27–28] upon molecular contact, and has been observed frequently in the interaction of DNA with porphyrins, phenanthroliens and salophen complex [29]. In contrast, the hypochromism is resulted from the tightenning of DNA duplex assembly [30–32].

In this study, UV-vis absorption spectra were recorded while increasing amount of the two compounds were added respectively to 0.02 mM CT-DNA solution. As shown in Fig. 6A, the maximum absorption of free CT-DNA was at 212 and 260 nm, and the absorption bands showed hyperchromism and a large red shift in λ_{max} upon the addition of different

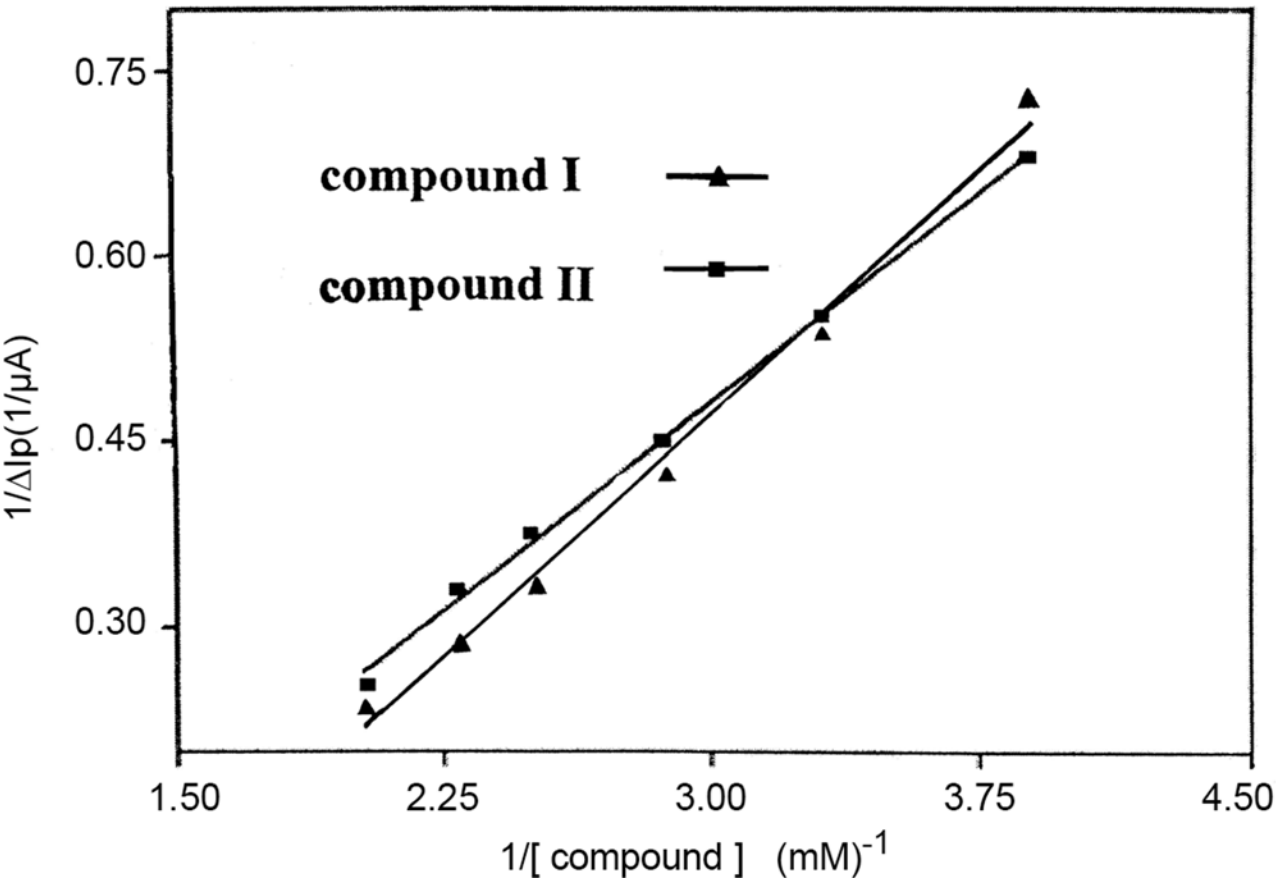

Fig 5. The relationship between $1/\Delta I_P$ and 1/C.

doi:10.1371/journal.pone.0120211.g005

concentrations of compound **I**. When the compound **I** concentration reached 0.08 mM, the hyperchromism was 49.4% and the red shift was 14–16 nm from band 260 nm. In contrast, as shown in Fig. 6B, the hyperchromism of 53.5% and the red shift of about 13 nm from band 260 nm were observed for compound **II**.

The hyperchromism appearing in absorbance around 258 nm without any hypsochromic effect, but with a bathochromic shift, can be attributed to the breaking of hydrogen bonds between complementary DNA strands, which resulting from intercalations of DNA with small molecules that leads the opening of DNA double helix [33–34]. The present results indicated the existence of strong intercalation of CT-DNA with the two compounds, this was consistent with a typical berberine-DNA intercalation which caused a hyperchromism of 35% with a red shift about 15 nm [35]. Further, the red shift might be ascribed to the intercalation of CT-DNA base pairs with aromatic chromophores of cymene and pyridyl [36–37], due to the decrease in energy gap between the highest and the lowest molecular orbitals (HUMO and LUMO) after CT-DNA binding with the compounds [38].

Conclusions

Cyclic voltammetry showed that the two compounds, [(η^6-*p*-cymene)Ru(L1)Cl_2 and (η^6-*p*-cymene)Ru(L1)Cl_2], were adsorbed by CT-DNA which was coated on gold electrode surface, the adsorption behavior was fit for *Langmuir* equation. Further, the hyperchromism of ultraviolet-visible absorbance spectra revealed the nature of the adsorption was intercalation of

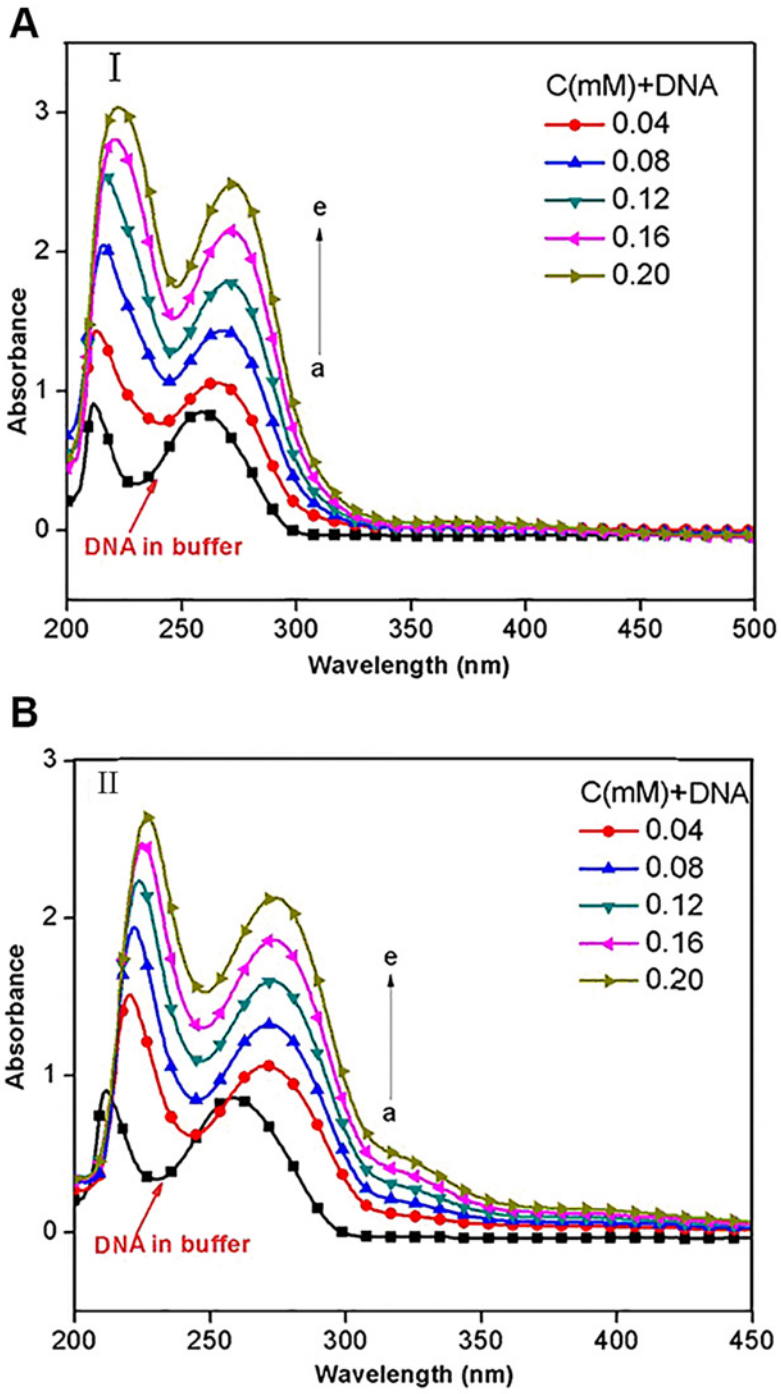

Fig 6. UV absorption spectra of CT-DNA (0.02mM) with various concentrations of compound I (A) and II (B).

doi:10.1371/journal.pone.0120211.g006

the two half-sandwich ruthenium(II) compounds with CT-DNA. The binding constant of compound I was approximately 2.1 times larger than that of compound II, which indicated that the compound I showed stronger CT-DNA binding ability than compound II. It might be expected boldly that compound I was a better antitumor agent than compound II.

Supporting Information

S1 Fig. The infrared spectrum of compound I.
(TIF)

S2 Fig. The ^{1}H-NMR spectrum of compound I.
(TIF)

S3 Fig. The ^{13}C-NMR spectrum of compound I.
(TIF)

S4 Fig. The infrared spectrum of compound II.
(TIF)

S5 Fig. The ^{1}H-NMR spectrum of compound II.
(TIF)

S6 Fig. The ^{13}C-NMR spectrum of compound II.
(TIF)

Acknowledgments

We thank Qian Miao for technical assistance, Shun Wang for many helpful discussions.

Author Contributions

Conceived and designed the experiments: ZMJ MLH ZJL YH DAQ. Performed the experiments: ZJL YH DAQ MLH ZMJ. Analyzed the data: ZMJ MLH ZJL YH DAQ. Contributed reagents/materials/analysis tools: MLH ZJL YH DAQ ZMJ. Wrote the paper: ZJL ZMJ MLH YH DAQ.

References

1. Ronconi L, Sadler PJ (2007) Using coordination chemistry to design new medicines. Coord Chem Rev 251: 1633–1648.
2. Ruiz J, Rodríguez V, Cutillas N, Espinosa A, Hannon MJ (2011) A potential ruthenium (II) antitumor complex bearing a lipophilic levonorgestrel group. Inorg Chem 50: 9164–9171. doi: 10.1021/ic201388n PMID: 21830785
3. Dougan SJ, Sadler PJ, Chimia (2007) The design of organometallic ruthenium arene anticancer agents. Int J Chem 61: 704–715.
4. Conejo-Garcia A, Schofield CJ (2005) A prodrug system for hydroxylamines based on esterase catalysis. Bioorg Med Chem Lett 15: 4004–4009. PMID: 15990293
5. Liu KG, Cai XQ, Li XC, Qin DA, Hu ML (2012) Arene-ruthenium(II) complexes containing 5-fluorouracil-1-methyl isonicotinate: Synthesis and characterization of their anticancer activity. Inorg Chim Acta 388: 78–83.
6. Shi Y, Guo CL, Sun YJ, Liu ZL, Xu FG, et al. (2011) Interaction between DNA and Microcystin-LR studied by Spectra Analysis and Atomic Force Microscopy. Biomacromol 12: 797–803.
7. Ding YH, Zhang L, Xie J, Guo R (2010) Binding characteristics and molecular mechanism of tnteraction between ionic liquid and DNA. J Phys Chem B 114: 2033–2043. doi: 10.1021/jp9104757 PMID: 20088558
8. Elder RM, Emrick T, Jayaraman A (2011) Understanding the effect of polylysine architecture on DNA binding using molecular dynamics simulations. Biomacromol 12: 3870–3879.
9. Campbell NH, Smith DL, Reszka AP, Neidle S, O'Hagan D (2011) Fluorine in medicinal chemistry: β-fluorination of peripheral pyrrolidiness attached to acridine ligands affects their interactions with G-quadruplex DNA. Org Biomol Chem 9: 1328–1331. doi: 10.1039/c0ob00886a PMID: 21221451
10. Akiyama Y, Ma Q, Edgar E, Laikhter A, Hecht SM (2008) Identification of strong DNA binding motifs for bleomycin. J Am Chem Soc 130: 9650–9651. doi: 10.1021/ja802905g PMID: 18597467
11. Lyles M. B, Cameron IL (2002) Interactions of the DNA intercalator acridine orange, with itself, with caffeine, and with double stranded DNA. Biophys Chem 96: 53–76. PMID: 11975993

12. Froehlich E, Mandeville JS, Kreplak L, Tajmir-Riahi HA (2011) Aggregation and particle formation of tRNA by dendrimers. Biomacromol 12: 2780–2787.
13. Liang MM, Liu XR, Liu GZ, Dou SP, Cheng DF, et al. (2010) Reducing the background fluorescence in mice receiving fluorophore/inhibitor DNA duplexes. Mol Pharm 8: 126–132. doi: 10.1021/mp100229z PMID: 21133414
14. Tong CL, Xiang GH, Bai Y (2010) Interaction of paraquat with calf thymus DNA: a terbium (III) fluorescence probe and multi-spectral study. J Agric Food Chem 58: 5257–5262. doi: 10.1021/jf1000748 PMID: 20402507
15. Sinha R, Saha I, Kumar GS (2011) Protoberberine alkaloids berberine, palmatine, and coralyne binding to poly(dT).poly(dA)*poly (dT) triplex: comparative structural aspects and energetics profiles of the interaction. Chem Biodiv 8: 1512–1528.
16. Bathaie SZ, Movahedi AAM, Saboury AA (1999) Energetic and binding properties of DNA upon interaction with dodecyl trimethylammonium bromide. Nucleic Acids Res 27: 1001–1005. PMID: 9927732
17. Yin P, Hu ML, Hu LC (2008) Synthesis, structural characterization and anticarcinogenic activity of a new Gly-Gly dipeptide derivative: Methyl 2-(2-(5-fluoro-2,4-dioxo-3,4-dihydropyrimidin-1-(2H)-yl) cetamido) acetate. J Mol Struct 882: 75–79.
18. Pang DW, Abruna HD (1998) Micromethod for the investigation of the interactions between DNA and redox-active molecules. Anal Chem 70: 3162–3169. PMID: 11013719
19. Jin BK, Ji XP, Nakamura T (2004) Voltammetric study of interaction of $Co(phen)_3^{3+}$ with DNA at gold nanoparticle self-assembly electrode. Electrochim Acta 50: 1049–1055.
20. Erkkila KE, Odom DT, Barton JK (1999) Recognition and reaction of metallointercalators with DNA. Chem Rev 99: 2777–2795. PMID: 11749500
21. Carter MT, Rodriguez M, Bard AJ (1989) Voltammetric studies of the interaction of metal chelates with DNA. 2. Tris-chelated complexes of cobalt(III) and iron(II) with 1,10-phenanthroline and 2,2'-bipyridine. J Am Chem Soc 111: 8901–8911.
22. Xu ZQ, Zhou B, Jiang FL, Dai J, Liu Y (2013) Interaction between a cationic porphyrin and ctDNA investigated by SPR, CV and UV—vis spectroscopy. Coll Surf B: Biointer 110: 321–326.
23. Kalanur SS, Seetharamappa J, Prashanth SN (2011) Interaction of an antidepressant buzepide methiodide with DNA immobilized on the glassy carbon electrode. Coll Surf B: Biointer 82: 438–442.
24. Liu SQ, Xu JJ, Chen HY (2004) A reversible adsorption—desorption interface of DNA based on nanosized zirconia and its application. Coll Surf B: Biointer 36: 155–159.
25. Li LL, Cao WQ, Zheng WJ, Fan CD, Chen TF (2012) Ruthenium complexes containing 2,6-bis(benzimidazolyl)pyridine derivatives induce cancer cell apoptosis by triggering DNA damage-mediated p53 phosphorylation. Dalton Transact 41: 12766–12772. doi: 10.1039/c2dt30665d PMID: 22968364
26. Li XC, Liu KG, Qin DA, Cheng CC, Chen BX, et al. (2012) Influence of bromoethyl group on biological activity of 5-fluorouracil prodrug: Insights from X-ray crystallography and molecular docking. J Mol Struct 1027: 104–110.
27. Hobro AJ, Rouhi M, Blanch EW, Conn GL (2007) Raman and raman optical activity (ROA) analysis of RNA structural motifs in Domain I of the EMCV IRES. Nucl Acids Res 35: 1169–1177. PMID: 17264119
28. Li Q, Yang P, Wang H, Guo M (1996) Diorganotin (IV) antitumor agent. $C_2H_5SnCl_2$ (phen)/nucleotides aquous and solid state coordination chemistry and its DNA binding studies J Inorg Biochem 64: 181–195. PMID: 8893519
29. Kashanian S, Gholivand MB, Ahmadi F, Taravati A, Hosseinzadeh Colagar A. (2007) DNA interaction with Al—N,N′-bis(salicylidene) 2,2′-phenylendiamine complex. Hosseinzadeh Colagar, Spectrochim. Acta Part A Mol Biomol Spectrosc 67: 472–478. PMID: 17011818
30. Rahban M, Divsalar A, Saboury AA, Golestani A (2010) Nanotoxicity and spectroscopy studies of silver nanoparticle: Calf thymus DNA and K562 as targets. J Phys Chem C 114: 5798–5803.
31. Wang BD, Yang ZY, Li TR (2006) Synthesis, characterization, and DNA-binding properties of the Ln(III) complexes with 6-hydroxy chromone-3-carbaldehyde-(2'-hydroxy) benzoyl hydrazine. Bioorg Med Chem 14: 6012–6021. PMID: 16781158
32. Wang BD, Yang ZY, Crewdson P, Wang DQ (2007) Synthesis, crystal structure and DNA-binding studies of the Ln(III) complex with 6-hydroxychromone-3-carbaldehyde benzoyl hydrazoneJ Inorg Biochem 101: 1492–1504. PMID: 17692381
33. Kashanian S, Gholivand MB, Ahmadi F, Ravan H (2008) Interaction of diazinon with DNA and the protective role of selenium in DNA damage. DNA Cell Biol 27: 325–332. doi: 10.1089/dna.2007.0718 PMID: 18447756
34. Arjmand F, Mohani B, Parveen S (2006) New dihydro O,O′-bis(salicylidene) 2,2′ aminobenzothiazolyl borate complexes: kinetic and voltammetric studies of dimethyltin copper complex with guanine, adenine, and calf thymus DNA. Bioinorg Chem Appl 2006: 1–10.

35. Li XL, Hu YJ, Wang H, Yu BQ, Yue HL (2012) Molecular spectroscopy evidence of berberine binding to DNA: comparative binding and thermodynamic profile of intercalation. Biomacromol 13: 873–880.

36. Arjmand F, Mohani B, Ahmad S (2005) Synthesis, antibacterial, antifungal activity and interaction of CT-DNA with a new benzimidazole derived Cu (II) complex. Eur J Med Chem 40: 1103–1110. PMID: 16006016

37. Baidini M, Ferrari MB, Bisceglie F, Pelosi G, Pinelli S, et al. (2003) Cu(II) complexes with heterocyclic substituted thiosemicarbazones: the case of 5-Formyluracil synthesis, characterization, X-ray structures, DNA interaction studies, and biological activity. Inorg Chem 42: 2049–2055. PMID: 12639140

38. Tan JH, Lu Y, Huang ZS, Gu LQ, Wu JY (2007) Spectroscopic studies of DNA binding modes of cation-substituted anthrapyrazoles derived from emodin. Eur J Inorg Chem 42:1169–1175.